or including asteroid fly-by, as Galileo and Cassini, will give a wealth of high-quality data on the asteroid population. Not a single close-up picture of a minor planet is yet available, but more information on asteroid rotations, shapes, poles and compositional types would provide interesting clues in understanding the role of collisions in producing the observed asteroid belt and more in general in the evolution of the solar system. Moreover, the data coming from *in situ* measurements will be detailed enough to clarify the nature and the interrelationships between small bodies populations, if any. Are some of the Earth-crossing asteroids nuclei of dead comets? Are the meteorites fragments of asteroids disrupted by mutual collisions, or are they the smallest size tail of the asteroidal size distribution? Are double or multiple systems present among asteroids?

In order to give an answer to these and other questions, while we wait for the results of the space missions, it is necessary to improve the number and quality of data on asteroids: unbiased and detailed Earth-based surveys, ISO orbiting observatory results and Space Telescope inputs will be the main sources of the future data. Embedded in the asteroid belt may be the clues that will help us to unravel the structure of the early solar system, to learn about the planetesimals and their evolution, and to fathom the mechanism by which planet-building was halted in this part of our planetary system.

Thanks to the ESO facilities, especially in the last five years, a lot of data, both physical and astrometric, were obtained on asteroids. Nevertheless, many unsolved problems still remain open and

among these the most intriguing are: (i) the knowledge of physical characteristics and origin of outer main belt and AAA asteroids, (ii) the collisional evolution of main belt objects and the related origin of dynamical families.

So far ESO has provided to the European asteroidal community small telescopes only (ESO 50-cm and 1-m, Bochum 61-cm, Danish 1.52-m and GPO). But in order to deepen our knowledge on asteroids and to solve, at least partially, the above-mentioned problems, the availability of larger instruments will be necessary, in particular, for photometric, polarimetric and spectroscopic observations.

Asteroids may be "small" and "near", nevertheless they deserve being investigated by means of large telescopes!

References

Barucci, M.A., Capria, M.T., Coradini, A., Fulchignoni, M.: 1987, *Icarus* **72,** 304.
Barucci, M.A., Capria, M.T., Harris, A.W., Fulchignoni, M.: 1989, *Icarus,* **83,** 325.
Binzel, R.P.: 1988, *Icarus* **73,** 303.
Capaccioni, F., Cerroni, P., Coradini, M., Di Martino, M., Farinella, P., Flamini, E., Martelli, G., Paolicchi, P., Smith, P.N., Woodward, A., Zappalà, V.: 1986, *Icarus* **66,** 487.
Chapman, C.R., Paolicchi, P., Zappalà, V., Binzel, R.P., Bell, J.F.: 1989, in *Asteroids II,* R.P. Binzel, T. Gehrels, M.S. Matthews eds., University of Arizona Press, Tucson, p. 386.
Davis, D.R., Weidenschilling, S.J., Farinella, P., Paolicchi, P., Binzel, R.P.: 1989, in *Asteroids II,* R.P. Binzel, T. Gehrels, M.S. Matthews eds., University of Arizona Press, Tucson, p. 805.
Davis, D.R., Chapman, C.R., Weidenschilling, S.J., Greenberg, R.: 1985, *Icarus* **62,** 30.
Dermott, S.F., Harris, A.W., Murray, C.D.: 1984, *Icarus* **57,** 14.

Drummond, J.D., Cocke, W.J., Hege, E.K., Strittmatter, P.A.: 1985, *Icarus* **61,** 132.
Farinella, P., Paolicchi, P., Zappalà, V.: 1981, *Icarus* **46,** 114.
Farinella, P., Paolicchi, P., Zappalà, V.: 1982, *Icarus* **52,** 409.
Fujiwara, A., Cerroni, P., Davis, D., Ryan, E., Di Martino, M., Holsapple, K., Housen, K.E.: 1989, in *Asteroids II,* R.P. Binzel, T. Gehrels, M.S. Matthews eds., University of Arizona Press, Tucson, p. 240.
Gradie, J., Veverka, J.: 1980, *Nature* **283,** 840.
Hartmann, W.K., Tholen, D.J., Cruikshank, D.P.: 1987, *Icarus* **69,** 33.
Magnusson, P.: 1983, in *Asteroids, Comets, Meteors,* C.-I. Lagerkvist and H. Rickman eds., Uppsala Universitet, Uppsala, p. 77.
Magnusson, P.: 1989, in *Asteroids II,* R.P. Binzel, T. Gehrels, M.S. Matthews eds., University of Arizona Press, Tucson, p. 1180.
Milani, A., Nobili, A.: 1985, *Astron. Astrophys.* **144,** 261.
Millis, R.L., Elliot, J.L.: 1979, in *Asteroids,* T. Gehrels ed., Univ. of Arizona Press, Tucson, p. 98.
Ostro, S.J.: 1989, in *Asteroids II,* R.P. Binzel, T. Gehrels, M.S. Matthews eds., University of Arizona Press, Tucson, p. 1920.
Ostro, S.J., Connelly, R.: 1984, *Icarus* **57,** 443.
Taylor, R.C.: 1979, in *Asteroids,* T. Gehrels ed., Univ. of Arizona Press, Tucson, p. 480.
Tholen, D.J.: 1984, PhD Thesis, Univ. of Arizona.
Tholen, D.J.: 1989, in *Asteroids II,* R.P. Binzel, T. Gehrels, M.S. Matthews eds., University of Arizona Press, Tucson, p. 1139.
Vilas, F., Smith, B.: 1985, *Icarus* **64,** 503.
Zappalà, V., Di Martino, M., Cacciatori, S.: 1983, *Icarus* **56,** 319.
Zappalà, V., Di Martino, M., Farinella, P., Paolicchi, P.: 1983, in *Asteorids, Comets, Meteors,* C.-I. Lagerkvist and H. Rickman eds., Uppsala Universitet, Uppsala, p. 73.
Zappalà, V., Farinella, P., Knežević, Z., Paolicchi, P.: 1984, *Icarus* **59,** 261.

The Dust Tail of Comet Wilson 1987 VII

G. CREMONESE, Osservatorio Astronomico, Padova, Italy
M. FULLE, Osservatorio Astronomico, Trieste, Italy

1. Introduction

Several photographic plates, both in red and blue light, were obtained by means of the ESO Schmidt camera to study the dust and plasma tails of Comet Wilson 1987 VII. All these plates were calibrated by means of calibration wedges and therefore are suitable for a quantitative analysis of the dust and ion tails. The pass-band of the emulsion-filter combination of red plates is from 630 to 700 nm, close to the R photometric system. We used plates 6810, 6829

and 6842 to study the dust environment of C/1987 VII before perihelion by means of the inverse numerical method which was successfully tested on C/1973 XII and C/1962 III (Fulle, 1989).

This model considers $N_t \times N_\mu \times N_s$ sample dust grains, where N_t is the number of samples in the time interval of dust ejection, N_μ is the number of samples in the sizes, and N_s is the number of grains of a fixed size uniformly distributed on a dust shell. It considers different ejection geometries for each of

which the ejection of dust is restricted to a cone of half width w with its symmetry axis pointing toward the Sun. The position of each grain at the observation is derived from its keplerian motion, then projected into the photographic plane coordinate system, so as to obtain the model distribution of the scattered light from the tail and the related kernel matrix A. The solutions are given by the minimization of the functional $[AF-I]^2 + \beta[BF]^2$, where A is the kernel matrix, I is the data vector containing the dust tail

Plate	Time	UT	r	Δ	α	Exp.	Emulsion	S_{10B}	R_{sky}
6810	Mar	27366	1.26	1.42	43°	20	098+RG630	–	–
6829	Apr	2368	1.23	1.24	48°	30	098+RG630	915 ± 15	20.38 ± 0.02
6842	Apr	7348	1.22	1.09	51°	30	098+RG630	750 ± 20	20.60 ± 0.04

TABLE 1: *Photographic data. Plate, serial number of the photographic plate. Time UT, time of mid-exposure. r, Δ, Sun-Comet and Earth-Comet distances (AU). α, Phase angle. Exp., exposure time (minutes). Emulsion, emulsion and filter combination. S_{10B}, sky background surface light intensity expressed in number of 10 R-magnitude stars per square degree. R_{sky}, sky background R-magnitude $arcsec^{-2}$.*

surface light intensities of the N_k images sampled in $N_N \times N_M$ points, B is a regularizing matrix weighted by β, and F is the solution vector sampled in $N_t \times N_\mu$ values, from which the dust number and mass loss rates and the time dependent and time averaged size distributions can be directly computed. Contrarily, the dust ejection velocity v(t) is required for the computation of the matrix A, so that it must be determined by means of a trial and error procedure. The regularizing weight β tunes the constraints to our ill-posed problem: when β increases, the instability of F decreases, but also the quality of the fit to the data. Therefore, the most probable dust velocity v(t) is defined as the function giving a stable and positive vector F for a regularizing weight β as small as possible.

2. Data Reduction

The plates were digitized adopting square scanning windows of 50 μm² and the photographic densities were transformed into intensity by means of the related calibration wedges. To perform the absolute calibration of the images, we selected three photometric fields from the first edition of the new Guide Star Photometric Catalogue (GSPC-I, Lasker, Sturch et al., 1988). Such fields were digitized by means of a square scanning window of 20 μm² and were linearized by means of the same calibration wedges used for the comet images. For each GSPC-I star of visual magnitude V, we obtained the red magnitude R following Johnson (1966) and measured the integrated intensity over a sky area covering the whole star trail and over a same area of sky background near the star trail, obtaining the sky background surface light intensity S_{10B} expressed in number of 10 R-magnitude stars per square degree (Table 1). The very small errors affecting the sky intensities refer to the fits to the measured star intensities, and not to systematic errors, which may well be larger and may have been introduced by the reciprocity effect of the plates (the exposure times of the stars and of the comet were obviously different, since the comet image is fixed, whereas the stars are trailed) and by the differences between
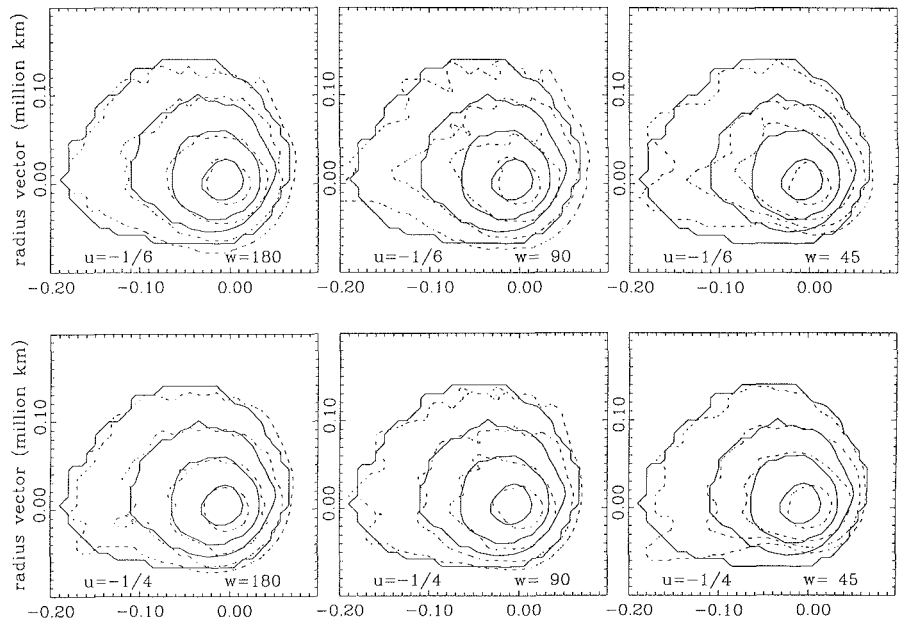
Figure 1: *Isophotes of the dust tail from image 6810 for the intensity levels 1.6, 2.4, 3.8 and 8.7 expressed in sky surface intensity units. The distances along the axes are expressed in 10^6 km units. Continuous lines: observed isophotes. Dashed lines: computed isophotes. w is the anisotropy parameter. u = δ log v(t, d)/δ log d (Table 2).*

our pass-band and the R photometric system.

3. Results

In Figure 1 we show the comparison between input image 6810 and the reconstruction of the same image by means of the solution F, which allows to test the accuracy of the solution itself and the stability of our constrained inverse problem. In Table 2 we show the parameters associated with the application of our method to the images of C/ 1987VII. For each parameter combination, we tested the number of trial velocity functions v(t) given in the table. The solutions concerning the dust ejection velocities, the range of diameters of the considered sample grains, the dust loss rates and the power index of the time-dependent size distribution are shown in

u	w	N_s	N_μ	N_t	N_t	N_μ	N_k	N_M	N_N	T	M	S
−1/6	180°	284	100	100	20	10	3	30	30	8	4.4	○
−1/6	90°	143	100	100	20	10	3	30	30	27	3.3	□
−1/6	45°	382	100	100	20	10	3	30	30	10	1.9	△
−1/4	180°	284	100	100	20	10	3	30	30	12	6.0	+
−1/4	90°	143	100	100	20	10	3	30	30	9	5.4	×
−1/4	45°	382	100	100	20	10	3	30	30	31	2.7	✳

TABLE 2: *Parameters of the model of Comet Wilson. u = δ log v(t, d)/δ log d. w, half width of the dust ejection cone: isotropic ejection (half width of π), hemispherical ejections (half width of π/2), and strongly anisotropic ejections (half width of π/4). N_s, N_μ, N_t, dust samples on a dust shell, in the modified size and in time. N_t, N_μ, samples of the solution in time and in the modified size. N_M, N_N, samples of the N_k source images in the M and N directions. T, number of test functions v(t). M, total ejected dust mass (10^{14} grams) for Ap(α) = 0.02. S, symbol in Fig. 2.*

Figure 2. The dust loss rates were computed adopting the albedo $Ap(\alpha) = 0.02$ (Hanner and Newburn, 1989, $43° < \alpha < 51°$, phase angle α in Table 1). The slow increase of the dust number loss rate is mostly due to the decreasing size interval which was considered. The mass loss rate related to isotropic dust ejections shows a wide maximum at $t \approx -120$ (days related to perihelion), that is at $r \approx 2.4$ AU, whereas the mass loss rate related to strongly anisotropic ejections is about constant. Large uncertainties of the loss rates are due to the poorly known albedo of large grains. The loss rates shown in Figure 2 are inversely proportional to the assumed value of $Ap(\alpha)$. The uncertainties of the dust bulk density are much less important. In fact the mass loss rate computed by means of dust tail analysis is independent of the dust density (Fulle, 1989), whereas the number loss rate is directly proportional to the square of dust density. For plates exposed to the red pass-band, the contamination by plasma (H_2O^+) is a concern along the prolonged radius vector. This is reflected in the residual instability of the solutions for $t > -60$, which explains the large dispersion of the mass loss rates and of the power index of the size distribution. However, plasma contamination to the left-hand side of the tails is very improbable, so that for $t < -60$ the solutions should be free of significant errors.

We find that C/1987VII produced more than 10^6 g s^{-1} of dust during two years before perihelion, and this may be related to its high relative luminosity at the first observations. Our results suggest that the mass loss rate does not increase close to perihelion, in agreement with the results of Hanner and Newburn (1989). The power index of the size distribution shows small variations. We find that its value is higher than -4, and this implies the release of very large grains. This fact is confirmed by the time
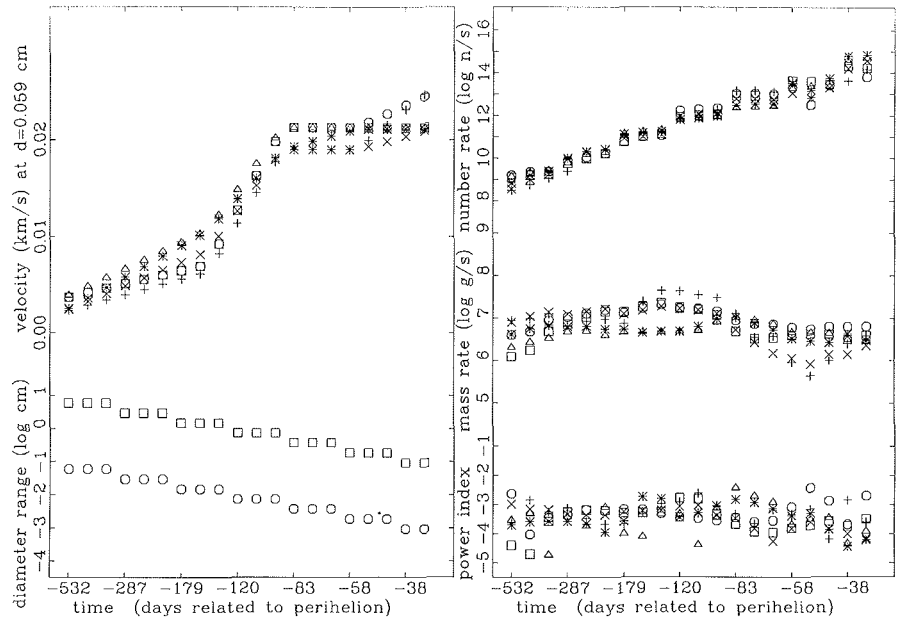
Figure 2: *Dust environment of Comet Wilson 1987 VII assuming the albedo $Ap(\alpha) = 0.02$: the dust loss rates (depending inversely on $Ap(\alpha)$), the dust ejection velocity, the power index of the time-dependent size distribution and the diameter interval to which all the solutions are related. The symbols are related to Table 2. The time sampling steps correspond to true anomaly steps of 5°.*

averaged size distribution, characterized by the very high power index of -3.0 ± 0.1. These results show that the dust loss of Comet Wilson 1987 VII was already significant at $r \approx 7$ AU, a Sun-Comet distance even larger than that observed for Comet Kohoutek $(r \approx 5$ AU). At these distances the gas production should be dominated by CO_2, and we observe also a maximum of the dust mass loss rate and a fast increase of the dust ejection velocity when the sublimation of H_2O becomes efficient.

Acknowledgements

References

Fulle, M., 1989, *Astron. Astrophys.* **217**, 283.
Johnson, H. L., 1966, *Annual Review Astron. Astrophys.* **4**, 193.
Lasker, B. M., C. R. Sturch, C. Lopez, A. D. Mallama, S. F. McLaughlin, J. L. Russell, W. Z. Wisniewsky, B. A. Gillespie, H. Jenkner, E. D. Siciliano, D. Kenny, J. H. Baumert, A. M. Goldberg, G. W. Henry, E. Kemper and M. J. Siegel 1988, *Astrophys. J. Suppl. Ser.* **68**, 1.
Hanner, M. S., and R. L. Newburn, 1989, *Astron. J.* **97**, 254.

Chiron's Blue Coma

R. M. WEST, ESO

The Most Distant Minor Planet Known

Among the nearly 4500 minor planets which have been numbered until now, (2060) Chiron is by far the most distant and certainly one of the most unusual. It moves in a rather eccentric orbit between the giant planets Saturn and Uranus and each revolution lasts just over 50 years.

Chiron was discovered in late 1977 by Charles Kowal of the Palomar Observatory. He found a slow-moving, 18-mag object on plates taken with the Palomar Schmidt telescope and within a few weeks, enough positions had been measured to compute a preliminary orbit. It was later identified on other photographic plates dating back to 1895, and soon the unique nature of Chiron was firmly established.

At the time of its discovery, Chiron was classified as a "minor planet", and it was obvious that it must be a very large one, in order to be so bright at this large distance. Depending on its ability to reflect sunlight (albedo), the diameter was estimated as somewhere between 100 and 250 kilometres. Kowal and other minor planet specialists felt that Chiron might be the first of a new family of minor planets, and it was inofficially de-